Journal of Molecular Structure 1081 (2015) 85–95

Contents lists available at ScienceDirect

Journal of Molecular Structure

journal homepage: www.elsevier.com/locate/molstruc

Synthesis, crystal structure, molecular docking and antimicrobial evaluation of new pyrrolo[3,2-c]pyridine derivatives

Gilish Jose [a], T.H. Suresha Kumara [a,e,*], Gopalpur Nagendrappa [a], H.B.V. Sowmya [a], Jerry P. Jasinski [b], Sean P. Millikan [b], Sunil S. More [c], Bhavya Janardhan [c], B.G. Harish [d], N. Chandrika [a]

[a] Postgraduate Department of Chemistry, Jain University, 52 Bellary Road, Hebbal, Bangalore, Karnataka 560024, India
[b] Department of Chemistry, Keene State College, Keene, NH 03435-2001, USA
[c] Department of Biochemistry, Center for Postgraduate Studies, Jain University, Bangalore, Karnataka 560011, India
[d] Department of Master of Computer Applications, Center for Postgraduate Studies, Visvesvaraya Technological University, Bangalore, Karnataka 560054, India
[e] Department of Chemistry, University B.D.T. College of Engineering, Davanagere, Karnataka 577004, India

HIGHLIGHTS

- A new series of pyrrolo[3,2-c]pyridine derivatives were designed and synthesized.
- The molecular docking of the GlcN-6-P synthase with target compounds was carried out.
- X-ray crystal structure determination and analysis of **6a** and **7c** were carried out.
- *In vitro* antibacterial and antifungal screening was carried out.
- Compound **7e** showed substantial antibacterial activity against *B. flexus*.

GRAPHICAL ABSTRACT

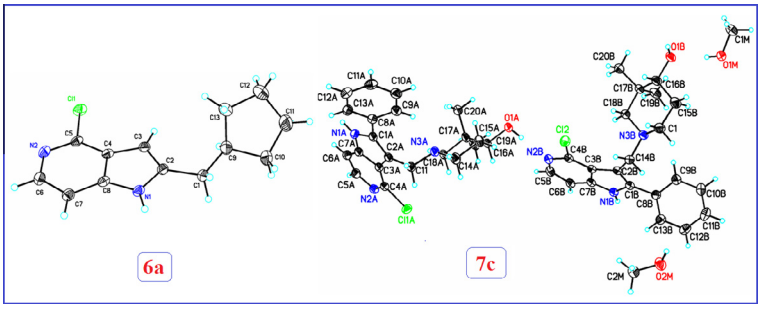

ARTICLE INFO

Article history:
Received 19 March 2014
Received in revised form 4 October 2014
Accepted 4 October 2014
Available online 12 October 2014

Keywords:
Antimicrobial activity
GlcN-6-P synthase
Pyrrolo[3,2-c]pyridine
X-ray crystallography

ABSTRACT

New antibacterial agents, pyrrolo[3,2-c]pyridine derivatives have been designed and synthesized. The structural considerations of the designed molecules were further supported by the docking study with GlcN-6-P synthase. The chemical structures of the new compounds were characterized by NMR, mass spectral analysis and elemental analysis. Single crystals of two compounds, $C_{13}H_{15}N_2Cl$ [**6a**] and $C_{21}H_{24}N_3OCl$, CH_4O [**7c**] were obtained allowing for structural analysis. [$C_{13}H_{15}N_2Cl$] monoclinic, $P2_1/c$, $a = 9.9763(6)$ Å, $b = 9.6777(6)$ Å, $c = 13.3002(9)$ Å, $\beta = 106.459(7)°$, $V = 1231.47(14)$ Å^3, $Z = 4$, $T = 173(2)$ K, μ(Cu Kα) = 2.522 mm^{-1}, $D_{calc} = 1.266$ g/mm^3, 7124 reflections, 2404 unique ($R_{int} = 0.0381$), $R_1 = 0.0420$ ($I > 2\sigma(I)$) and $wR_2 = 0.1254$ (all data). [$C_{21}H_{24}N_3OCl$, CH_4O] triclinic, $P-1$, $a = 10.1478(7)$ Å, $b = 12.0945(8)$ Å, $c = 18.3244(10)$ Å, $\alpha = 104.369(5)°$, $\beta = 90.766(5)°$, $\gamma = 99.235(6)°$, $V = 2147.1(2)$ Å^3, $Z = 4$, $T = 173(2)$ K, μ(Cu Kα) = 1.744 mm^{-1}, $D_{calc} = 1.243$ g/mm^3, 14238 reflections, 8297 unique ($R_{int} = 0.0330$), $R_1 = 0.0578$ ($I > 2\sigma(I)$) and $wR_2 = 0.1773$ (all data). The *in vitro* antimicrobial activities of the compounds were conducted against various Gram-negative, Gram-positive bacteria and fungi. Amongst the tested compounds **7e** displayed promising antibacterial activity against Gram-positive bacteria *Bacillus flexus* compared to antibiotic Amoxicillin.

* Corresponding author at: Department of Chemistry, University B.D.T. College of Engineering, Davanagere, Karnataka 577004, India. Tel.: +91 9916588466.
E-mail addresses: suresha.kumara@gmail.com, suresha.kumara@rediffmail.com (T.H. Suresha Kumara).

http://dx.doi.org/10.1016/j.molstruc.2014.10.006
0022-2860/

Introduction

The pyrrolopyridine motifs are a growing class of heterocyclic scaffold present in many natural and unnatural compounds with significant biological applications. For example, the natural product variolin B **1** (Fig. 1) is a promising anticancer agent [1]. Other examples include the synthetic pyrrolopyridine derivative diazarebeccamycin **2** is a potent anticancer agent [2], pyrrolo[2,3-c]pyridine **3** which has demonstrated activity as an inhibitor of HIV-1 attachment to $CD4^+$ T cells [3] and pyrrolo[2,3-b]pyridine **4** is a potent p38 kinase inhibitor [4]. Pyrrolopyridines also posses significant biological applications such as antimicrobial [5–9], analgesic [10], antimalarial [11], antiproliferative [12], antihypertensive [13], cannabinoid activity [14,15] and Factor VIIa inhibitors [16]. As a result of our considerable interest in the synthesis of pyridine-containing compounds and their antimicrobial activity [17], we initiated a programme directed towards the synthesis of new pyrrolopyridine compounds.

The emergence of multiple drug resistant microorganisms has caused major health concern worldwide. Infections caused by bacteria and fungi remain a major health concern due to the development of resistance to existing antimicrobial agents [18–21]. Therefore, there is an increasing need to design and synthesize new antimicrobial agents with a broad spectrum of activities. On the basis of potential antimicrobial properties of pyrrolopyridine compounds [5–9], we earmarked to design new pyrrolopyridine derivatives anticipating enhanced antimicrobial activity. The new pyrrolopyridines were designed based on the assumptions of Lipinski rule to fulfil the drug likeness properties of the molecules. The structural considerations of the designed molecules were further supported by the docking study with target enzyme, L-glutamine: D-fructose-6-phosphate amidotransferase (EC 2.6.1.16), known under the trivial name of glucosamine-6-phosphatesynthase (GlcN-6-P synthase), as such new target for antimicrobial studies [22]. We report herein, synthesis, X-ray crystal structure analysis, molecular docking and antimicrobial evaluation of new pyrrolo[3,2-c]pyridine derivatives.

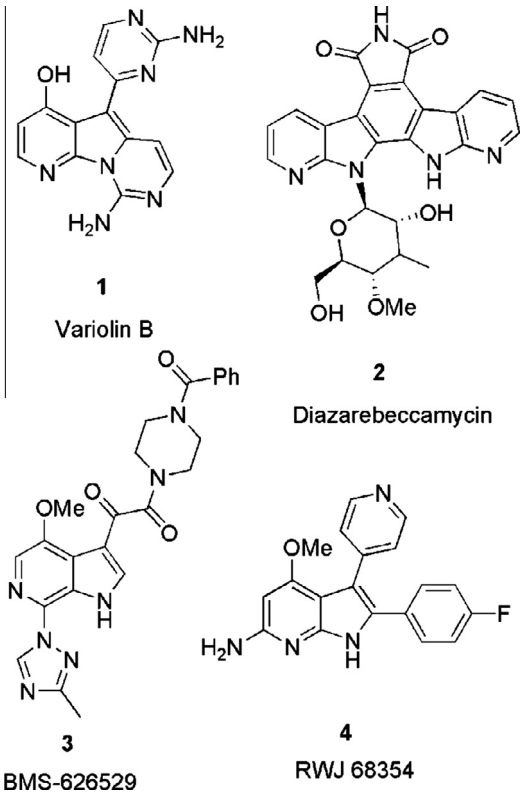

Fig. 1. Examples of biologically active pyrrolopyridines.

Experimental section

General methods: All chemicals and solvents were purchased from commercial suppliers. All reactions were performed under an inert atmosphere of dry nitrogen using dry solvents. The progress of the reactions was monitored by using Si gel 60 F_{254} thin layer chromatography plates and spots were detected by UV/254 nm. Compounds were purified by column chromatography on silica gel 230–400 using petether/ethyl acetate or dichloromethane/methanol solvent mixtures as eluent. All the compounds were characterized by ^{1}H NMR, ^{13}C NMR, LCMS and elemental analysis. Melting points of the samples were determined in open capillary tubes using Buchi Melting point B-540 apparatus and are uncorrected. ^{1}H and ^{13}C NMR spectra were recorded on a Bruker NMR spectrometer (400 and 100 MHz, respectively) using deuterated DMSO as solvent with TMS as internal standard. The mass recorded in Agilent LCMS 1100 series instrument using API-ES positive-ion mode and negative-ion mode. The CHN analysis was recorded in an Elementar vario MICRO cube.

*Experimental procedure for the synthesis of 2-chloro-3-iodopyridin-4-amine (**2**) [17]*

A mixture of 2-chloro-4-amino pyridine **1** (20 g, 0.15 mol), potassium acetate (22.9 g, 0.23 mol) and ICl (27.7 g, 0.17 mol) in glacial acetic acid (200 mL) was heated to 70 °C for 4 h. After completion of the reaction, the solvent was concentrated under reduced pressure. The residue was neutralized with 10% $NaHCO_3$ solution (250 mL) and extracted with two 300-mL portions of EtOAc. The combined organic extracts were washed with brine (200 mL) and dried over anhydrous Na_2SO_4. The solvent was removed in vacuum. The crude product showed a mixture of iodopyridines **2**, **3** and **4** in the ratio 45:45:10. The required compound **2** (elution 3) was isolated via normal phase preparative HPLC (mobile phase: 60:40, 0.1% TFA in hexane-IPA; column: SunFire Silica 19 × 150 mm, 5 μm; Flow rate: 18.0 mL/min) in 49.7% yield (19.7 g) as an off white solid; mp 102.9–104.1 °C; ^{1}H NMR (400 MHz, DMSO-D_6): δ 7.73 (d, J = 4.0 Hz, 1H), 6.52 (d, J = 4.0 Hz, 1H), 6.50 (s, 2H); MS (*m/z*): 255.0 $[M+H]^+$. Anal. calcd. for $C_5H_4ClIN_2$: C, 23.60; H, 1.58; N, 11.01; found: C, 23.59; H, 1.578; N, 10.99.

*General experimental procedure for the synthesis of **6a–c***

In a Schlenk tube, compound **2** (11.79 mmol), Copper (1) iodide (0.59 mmol), triethylamine (35.37 mmol) and alkyne (14.15 mmol) were mixed in THF (30 mL). The Schlenk tube was capped with a rubber septum, evacuated and backfilled with argon (this sequence was carried out four times). Bis(triphenylphosphine)palladium(II) dichloride (0.58 mmol) was added and the Schlenk tube was sealed with a Teflon screw cap. The reaction mixture was refluxed for 1 h. After completion of the reaction, the reaction mixture was filtered through a thin pad of celite (eluted with CH_2Cl_2) and the eluent was concentrated under reduced pressure. The solvent was removed under reduced pressure and the crude product was passed through a small plug of silica (eluted with CH_2Cl_2) and the eluent was concentrated under reduced pressure to afford **5a–c**. The crude product was as such taken for the next step without purification.

In an oven-dried RB flask, compound **5a–c** (8.04 mmol) and potassium tert-butoxide (16.08 mmol) were mixed in NMP

(20 mL). The reaction mixture was heated at 100 °C for 1 h. After completion of the reaction, the reaction mixture was diluted with DCM (60 mL) and the organic layer was washed with water (30 mL × 3) and brine (30 mL). The organic layer was separated, dried over anhydrous Na_2SO_4 and concentrated. The crude product was purified by silica gel column chromatography to provide **6a**–**c**.

*4-Chloro-2-(cyclopentylmethyl)-1H-pyrrolo[3,2-c]pyridine (**6a**)*

Pale yellow solid (82%); mp 145.8–148.7 °C; ^{1}H NMR (400 MHz, DMSO-D_6): δ 11.73 (s, 1H), 7.87 (d, *J* = 5.6 Hz, 1H), 7.29–7.28 (m, 1H), 6.24 (s, 1H), 2.72 (d, *J* = 7.5 Hz, 2H), 2.26–2.22 (m, 1H), 1.72–1.67 (m, 2H), 1.66–1.54 (m, 2H), 1.53–1.47 (m, 2H), 1.23–1.18 (m, 2H); ^{13}C NMR (100 MHz, DMSO-D_6): δ 142.4, 140.9, 140.6, 138.5, 123.2, 106.3, 97.2, 38.9, 33.4, 31.9, 24.5; MS (*m/z*): 235.0 $[M+H]^+$; Anal. calcd. for $C_{13}H_{15}ClN_2$: C, 66.52; H, 6.44; N, 11.93; found: C, 66.50; H, 6.447; N, 11.92.

*4-Chloro-2-phenyl-1H-pyrrolo[3,2-c]pyridine (**6b**)*

Pale yellow solid (87%); mp 166.8–169.7 °C; ^{1}H NMR (400 MHz, DMSO-D_6): δ 12.36 (s, 1H), 7.97–7.93 (m, 3H), 7.50 (q, *J* = 7.9 Hz, 2H), 7.41–7.37 (m, 2H), 7.03 (s, 1H); ^{13}C NMR (100 MHz, DMSO-D_6): δ 142.0, 141.7, 139.8, 139.6, 130.7, 129.0, 128.5, 125.6, 123.7, 106.8, 97.0; MS (*m/z*): 229.0 $[M+H]^+$; Anal. calcd. for $C_{13}H_9ClN_2$: C, 68.28; H, 3.97; N, 12.25; found: C, 68.30; H, 3.964; N, 12.24.

*4-Chloro-2-(cyclohexylmethyl)-1H-pyrrolo[3,2-c]pyridine (**6c**)*

Pale yellow solid (80%); mp 135.8–138.6 °C; ^{1}H NMR (400 MHz, DMSO-D_6): δ 11.72 (s, 1H), 7.86 (d, *J* = 5.5 Hz, 1H), 7.29–7.27 (m, 1H), 6.22 (s, 1H), 2.61 (d, *J* = 6.8 Hz, 2H), 1.70–1.57 (m, 6H), 1.22–1.15 (m, 3H), 1.14–0.98 (m, 2H); ^{13}C NMR (100 MHz, DMSO-D_6): δ 142.4, 141.4, 140.6, 138.4, 123.1, 106.3, 97.6, 37.3, 35.1, 32.4, 25.8, 25.5; MS (*m/z*): 249.0 $[M+H]^+$; Anal. calcd. for $C_{14}H_{17}ClN_2$: C, 67.60; H, 6.89; N, 11.26; found: C, 67.62; H, 6.882; N, 11.28.

*General experimental procedure for the synthesis of **7a**–**f***

4-Chloro-2-(cyclohexylmethyl)-3-(morpholinomethyl)-1H-pyrrolo[3,2-c]pyridine (**7d**) as an example: In an oven-dried RB flask, compound **6c** (250 mg, 1.01 mmol) and formaldehyde solution, 37–41 wt.% in water (0.15 mL, 2.02 mmol) were mixed in glacial acetic acid (5 mL). Morpholine (220.4 mg, 2.53 mmol) was added drop wise at 0 °C. The resulting mixture was stirred at room temperature for 12 h. After completion of the reaction, the excess solvent was evaporated to dryness under reduced pressure. The residue was neutralized with 10% $NaHCO_3$ solution, the solid formed was collected by filtration, washed with water and dried. The crude product was purified by silica gel column chromatography to provide title compound.

*4-Chloro-2-(cyclopentylmethyl)-3-((4-isopropylpiperazin-1-yl)methyl)-1H-pyrrolo[3,2-c]pyridine (**7a**)*

Off white solid (93%); mp 195.8–198.7 °C; ^{1}H NMR (400 MHz, DMSO-D_6): δ 11.63 (s, 1H), 7.84 (d, *J* = 5.6 Hz, 1H), 7.25 (d, *J* = 5.6 Hz, 1H), 3.66 (s, 2H), 2.72 (d, *J* = 7.6 Hz, 2H), 2.56–2.53 (m, 1H), 2.45–2.25 (m, 9H), 1.70–1.57 (m, 4H), 1.53–1.44 (m, 2H), 1.28–1.17 (m, 2H), 0.90 (d, *J* = 6.4 Hz, 6H); ^{13}C NMR (100 MHz, DMSO-D_6): δ 142.4, 141.1, 140.7, 138.1, 121.7, 106.9, 106.2, 53.5, 52.6, 50.6, 48.0, 38.9, 31.7, 31.2, 24.4, 18.1; MS (*m/z*): 375.2 $[M+H]^+$; Anal. calcd. for $C_{21}H_{31}ClN_4$: C, 67.27; H, 8.33; N, 14.94; found: C, 67.26; H, 8.324; N, 14.93.

*1-((4-Chloro-2-phenyl-1H-pyrrolo[3,2-c]pyridin-3-yl)methyl)piperidin-4-ol (**7b**)*

White solid (90%); mp 206.8–209.7 °C; ^{1}H NMR (400 MHz, DMSO-D_6): δ 12.17 (s, 1H), 7.95 (d, *J* = 5.6 Hz, 1H), 7.90 (d, *J* = 7.2 Hz, 2H), 7.52 (t, *J* = 7.6 Hz, 2H), 7.43 (t, *J* = 7.6 Hz, 1H), 7.37 (d, *J* = 5.2 Hz, 1H), 4.46 (d, *J* = 3.6 Hz, 1H), 3.77 (s, 2H), 3.42–3.41 (m, 1H), 2.71–2.68 (m, 2H), 2.15–2.10 (m, 2H), 1.65–1.63 (m, 2H), 1.34–1.26 (m, 2H); ^{13}C NMR (100 MHz, DMSO-D_6): δ 142.0, 141.2, 139.5, 139.1, 131.6, 129.1, 128.5, 128.3, 122.3, 108.8, 106.7, 66.4, 50.1, 50.0, 34.6; MS (*m/z*): 342.2 $[M+H]^+$; Anal. calcd. for $C_{19}H_{20}ClN_3O$: C, 66.76; H, 5.90; N, 12.29; found: C, 66.74; H, 5.893; N, 12.28.

*1-((4-Chloro-2-phenyl-1H-pyrrolo[3,2-c]pyridin-3-yl)methyl)-3,3-dimethylpiperidin-4-ol (**7c**)*

White solid (94%); mp 186.7–189.6 °C; ^{1}H NMR (400 MHz, DMSO-D_6): δ 12.17 (s, 1H), 7.95 (t, *J* = 5.2 Hz, 3H), 7.50 (t, *J* = 7.6 Hz, 2H), 7.42 (t, *J* = 7.2 Hz, 1H), 7.37 (d, *J* = 5.6 Hz, 1H), 4.36 (d, *J* = 4.8 Hz, 1H), 4.07 (q, *J* = 5.2 Hz, 1H), 3.77–3.65 (m, 2H), 3.17 (d, *J* = 5.2 Hz, 1H), 3.09–3.05 (m, 1H), 2.42 (d, *J* = 10.8 Hz, 1H), 1.90 (d, *J* = 11.2 Hz, 1H), 1.52–1.48 (m, 1H), 1.43–1.33 (m, 1H), 0.83 (d, *J* = 7.2 Hz, 6H); ^{13}C NMR (100 MHz, DMSO-D_6): δ 142.0, 141.1, 139.4, 139.0, 131.5, 129.0, 128.4, 128.3, 122.3, 108.6, 106.8, 73.8, 63.7, 50.1, 48.5, 35.6, 30.7, 25.9; MS (*m/z*): 375.2 $[M+H]^+$; Anal. calcd. for $C_{21}H_{24}ClN_3O$: C, 68.19; H, 6.54; N, 11.36; found: C, 68.20; H, 6.546; N, 11.35.

*4-Chloro-2-(cyclohexylmethyl)-3-(morpholinomethyl)-1H-pyrrolo[3,2-c]pyridine (**7d**)*

White solid (89%); mp 105.9–108.7 °C; ^{1}H NMR (400 MHz, DMSO-D_6): δ 11.67 (s, 1H), 7.84 (d, *J* = 5.6 Hz, 1H), 7.26 (d, *J* = 5.6 Hz, 1H), 3.69 (s, 2H), 3.56–3.44 (m, 4H), 2.63 (d, *J* = 6.8 Hz, 2H), 2.45–2.30 (m, 4H), 1.76–1.71 (m, 1H), 1.64–1.56 (m, 4H), 1.16–1.09 (m, 4H), 1.02–0.93 (m, 2H); ^{13}C NMR (100 MHz, DMSO-D_6): δ 141.1, 140.7, 140.4, 138.2, 121.7, 106.8, 106.2, 66.3, 52.8, 51.0, 37.6, 33.1, 32.6, 25.8, 25.7; MS (*m/z*): 348.2 $[M+H]^+$; Anal. calcd. for $C_{19}H_{26}ClN_3O$: C, 65.60; H, 7.53; N, 12.08; found: C, 65.61; H, 7.534; N, 12.07.

*4-Chloro-2-(cyclohexylmethyl)-3-((4-methylpiperazin-1-yl)methyl)-1H-pyrrolo[3,2-c]pyridine (**7e**)*

Off white solid (91%); mp 115.9–118.6 °C; ^{1}H NMR (400 MHz, DMSO-D_6): δ 11.62 (s, 1H), 7.84 (d, *J* = 5.6 Hz, 1H), 7.25 (d, *J* = 5.6 Hz, 1H), 3.66 (s, 2H), 2.62 (d, *J* = 7.2 Hz, 2H), 2.46–2.33 (m, 4H), 2.29–2.15 (m, 4H), 2.09 (s, 3H), 1.76–1.71 (m, 1H), 1.69–1.63 (m, 2H), 1.62–1.53 (m, 3H), 1.21–1.09 (m, 3H), 1.02–0.93 (m, 2H); ^{13}C NMR (100 MHz, DMSO-D_6): δ 141.1, 140.6, 140.3, 138.2, 121.7, 107.3, 106.2, 54.8, 52.1, 50.6, 45.7, 37.6, 33.2, 32.6, 25.9, 25.7; MS (*m/z*): 361.2 $[M+H]^+$; Anal. calcd. for $C_{20}H_{29}ClN_4$: C, 66.56; H, 8.10; N, 15.52; found: C, 66.59; H, 8.111; N, 15.53.

*N-benzyl-N-((4-chloro-2-(cyclohexylmethyl)-1H-pyrrolo[3,2-c]pyridin-3-yl)methyl) ethanamine (**7f**)*

Off white solid (88%); mp 155.6–158.5 °C; ^{1}H NMR (400 MHz, DMSO-D_6): δ 11.63 (s, 1H), 7.83 (d, *J* = 5.6 Hz, 1H), 7.25–7.23 (m, 5H), 7.16 (s, 1H), 3.81 (s, 2H), 3.49 (s, 2H), 2.60 (d, *J* = 7.2 Hz, 2H), 2.45–2.40 (m, 2H), 1.75–1.67 (m, 1H), 1.66–1.55 (m, 3H), 1.54–1.50 (m, 2H), 1.17–1.05 (m, 3H), 0.99–0.95 (m, 3H), 0.92–0.86 (m, 2H); ^{13}C NMR (100 MHz, DMSO-D_6): δ 140.9, 140.7, 140.6, 140.1, 138.0, 128.5, 127.9, 126.5, 121.9, 107.9, 106.3, 56.8, 46.6, 46.3, 37.4, 33.1, 32.5, 25.8, 25.6, 11.6; MS (*m/z*): 396.2 $[M+H]^+$; Anal. calcd. for $C_{24}H_{30}ClN_3$: C, 72.80; H, 7.64; N, 10.61; found: C, 72.81; H, 7.647; N, 10.60.

X-ray crystallography

The structures of **6a** and **7c** were unequivocally established by X-ray crystallographic analysis. A suitable crystal was selected and analyzed on an Agilent, Eos, Gemini diffractometer. The crystal was kept at 173(2) K during data collection. Using Olex2 [23], the

structure were solved the Superflip [24] structure solution program using Charge Flipping and refined with the ShelXL [25] refinement package using Least Squares minimization.

*Crystal structure determination of [**6a**]*

The X-ray crystallographic analysis of **6a** was carried out on an off white crystal, with dimensions 0.34 mm × 0.18 mm × 0.08 mm, grown from the slow evaporation of methanol at room temperature. Crystal data for **6a**, $C_{13}H_{15}N_2Cl$ (M = 234.72): monoclinic, space group $P2_1/c$, a = 9.9763(6) Å, b = 9.6777(6) Å, c = 13.3002(9) Å, β = 106.459(7)°, V = 1231.47(14) Å^3, Z = 4, T = 173(2) K, μ(Cu Kα) = 2.522 mm^{-1}, D_{calc} = 1.266 g/mm^3, 7124 reflections measured (9.244 ⩽ 2Θ ⩽ 145.144), 2404 unique (R_{int} = 0.0381) which were used in all calculations. The final R_1 was 0.0420 ($I > 2\sigma(I)$) and wR_2 was 0.1254 (all data) (Table 1).

Table 1
Crystal data and structure refinement for **6a** and **7c**.

Identification code	**6a**	**7c**
Empirical formula	$C_{13}H_{15}N_2Cl$	$C_{21}H_{24}N_3OCl$, CH_4O
Formula weight	234.72	369.88
Temperature/K	173(2)	173(2)
Crystal system	Monoclinic	Triclinic
Space group	$P2_1/c$	$P-1$
a (Å)	9.9763(6)	10.1478(7)
b (Å)	9.6777(6)	12.0945(8)
c (Å)	13.3002(9)	18.3244(10)
α (°)	90	104.369(5)
β (°)	106.459(7)	90.766(5)
γ (°)	90	99.235(6)
Volume (Å^3)	1231.47(14)	2147.1(2)
Z	4	4
ρ_{calc} (mg/mm^3)	1.266	1.243
m (mm^{-1})	2.522	1.744
F(000)	496.0	856.0
Crystal size (mm^3)	0.34 × 0.18 × 0.08	0.38 × 0.34 × 0.22
2Θ range for data collection	9.244–145.144°	7.656–145.27°
Index ranges	$-12 \leqslant h \leqslant 9$, $-10 \leqslant k \leqslant 11$, $-16 \leqslant l \leqslant 16$	$-10 \leqslant h \leqslant 12$, $-14 \leqslant k \leqslant 12$, $-22 \leqslant l \leqslant 22$
Reflections collected	7124	14238
Independent reflections	2404[R(int) = 0.0381]	8297[R(int) = 0.0330]
Data/restraints/parameters	2404/0/145	8297/0/527
Goodness-of-fit on F^2	1.054	1.033
Final R indexes [$I \geqslant 2\sigma(I)$]	R_1 = 0.0420, wR_2 = 0.1139	R_1 = 0.0578, wR_2 = 0.1580
Final R indexes [all data]	R_1 = 0.0530, wR_2 = 0.1254	R_1 = 0.0716, wR_2 = 0.1773
Largest diff. peak/hole (e Å^{-3})	0.25/−0.20	0.50/−0.32

*Crystal structure determination of [**7c**]*

The X-ray crystallographic analysis of **7c** was carried out on a white crystal, with dimensions 0.38 mm × 0.34 mm × 0.22 mm, grown from the slow evaporation of a dichloromethane and methanol solvent mixture at room temperature. Crystal data for **7c**, $C_{21}H_{24}N_3OCl$, CH_4O, (M = 401.92): triclinic, space group $P-1$, a = 10.1478(7) Å, b = 12.0945(8) Å, c = 18.3244(10) Å, β = 90.766(5)°, V = 2147.1(2) Å^3, Z = 4, T = 173(2) K, μ(Cu Kα) = 1.744 mm^{-1}, D_{calc} = 1.243 g/mm^3, 14238 reflections measured (7.656 ⩽ 2Θ ⩽ 145.27), 8297 unique (R_{int} = 0.0330) which were used in all calculations. The final R_1 was 0.0578 ($I > 2\sigma(I)$) and wR_2 was 0.1773 (all data) (Table 1).

In vitro antimicrobial procedure

All the newly synthesized compounds were evaluated *in vitro* for their antimicrobial activity. The antimicrobial activities are carried out against Gram-positive bacteria *Bacillus flexus*, Gram-negative bacteria *Pseudomonas* spp., fungal stains *Scopulariopsis* spp. and *Aspergillus tereus* using the nutrient agar disc diffusion method [26]. The synthesized compounds were dissolved in DMSO to get stock solutions. The antimicrobial activity was determined by measuring of the inhibition zone, after 20 h of incubation at 37 °C for bacterial strains and 4 days at 37 °C for fungal strains. The diameter of inhibition zones (in mm) was determined and the data were statistically evaluated by Turkey's fair wise comparison test. Commercial bactericide Amoxicillin was used as standard (100 μg per 100 μL of sterilized distilled water) concomitantly with the test samples.

MIC values for the synthesized compounds were determined by using broth microdilution [27]. Standard and isolated strain of *B. flexus* was used to determine the antibacterial activity as the compounds showed the activity against the above mentioned organism. Amoxicillin was used as the reference. The bacterium was cultivated in Mueller–Hinton agar and was diluted with Mueller–Hinton broth. The synthesized compounds and references were dissolved in DMSO at a concentration of 1000 μg/mL. Two fold

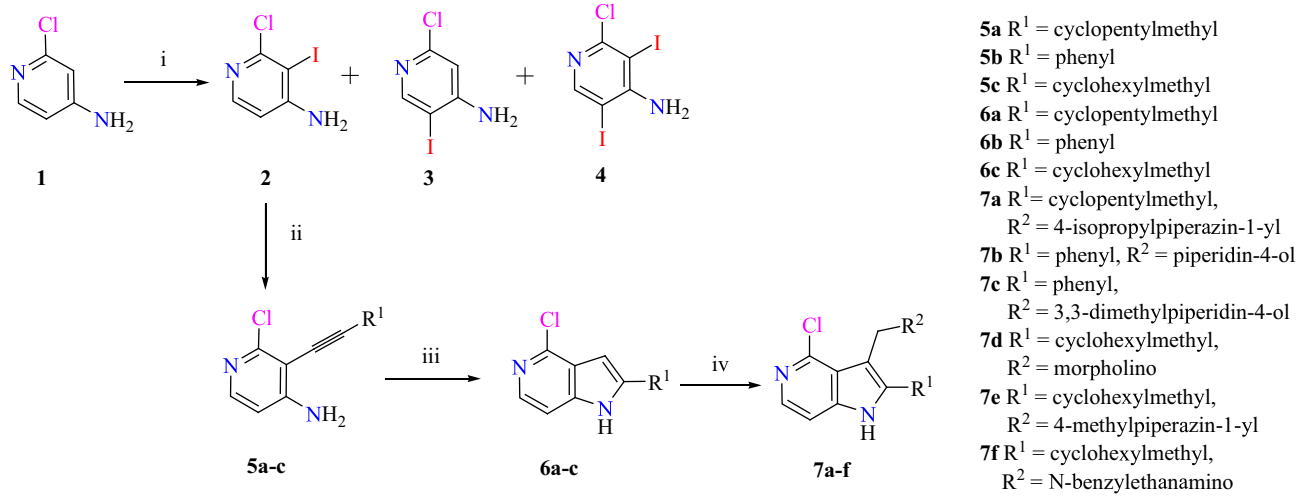

5a R^1 = cyclopentylmethyl
5b R^1 = phenyl
5c R^1 = cyclohexylmethyl
6a R^1 = cyclopentylmethyl
6b R^1 = phenyl
6c R^1 = cyclohexylmethyl
7a R^1= cyclopentylmethyl, R^2 = 4-isopropylpiperazin-1-yl
7b R^1 = phenyl, R^2 = piperidin-4-ol
7c R^1 = phenyl, R^2 = 3,3-dimethylpiperidin-4-ol
7d R^1 = cyclohexylmethyl, R^2 = morpholino
7e R^1 = cyclohexylmethyl, R^2 = 4-methylpiperazin-1-yl
7f R^1 = cyclohexylmethyl, R^2 = N-benzylethanamino

Scheme 1. Synthesis of pyrrolo[3,2-c]pyridine derivatives; (i) ICl and KOAc in glacial AcOH at 70 °C, 4 h; (ii) R^1-acetylene, CuI, $PdCl_2(PPh_3)_2$, Et_3N in THF, reflux, 1 h; (iii) KOt-Bu in NMP at 100 °C, 1 h; (iv) HCHO, R^2-secondary amine in glacial AcOH, rt, 12 h.

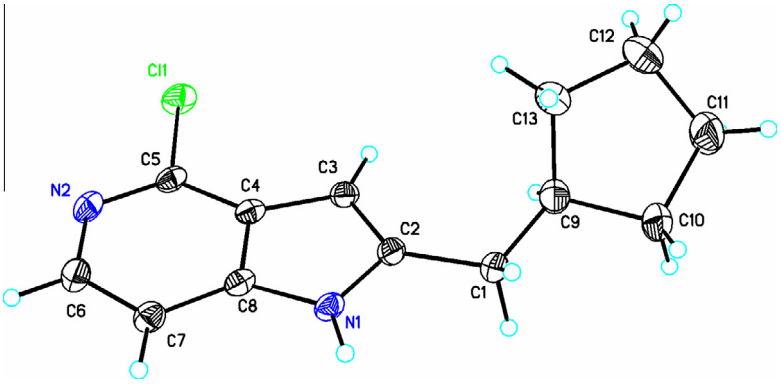

Fig. 2. Molecular structure of $C_{13}H_{15}N_2Cl$ (**6a**) showing the atom labeling scheme with two molecules in the asymmetric unit and 30% probability displacement ellipsoids.

Table 2
Selected Crystal Bond lengths (Å), Bond angles (°), and Torsion angles (°) for $C_{13}H_{15}N_2Cl$ (**6a**).

$C_{13}H_{15}N_2Cl$			
Cl1---C5	1.7476(19)	C1---C2	1.501(3)
N1---C2	1.377(2)	C1---C9	1.503(3)
N1---C8	1.358(2)	C2---C3	1.360(3)
N2---C5	1.316(3)	C3---C4	1.425(3)
N2---C6	1.359(3)	C4---C5	1.387(2)
$C_{13}H_{15}N_2Cl$			
C8---N1---C2	109.44(15)	C3---C2---C1	132.29(19)
C5---N2---C6	117.28(16)	C2---C3---C4	106.56(17)
C2---C1---C9	116.45(17)	C5---C4---C3	137.33(18)
N1---C2---C1	117.90(17)	C5---C4---C8	115.49(17)
C3---C2---N1	109.80(16)	C8---C4---C3	107.17(16)
$C_{13}H_{15}N_2Cl$			
N1---C2---C3---C4	0.0(2)	C2---N1---C8---C4	0.12(19)
N2---C6---C7---C8	-0.4(3)	C2---N1---C8---C7	-179.36(19)
C1---C2---C3---C4	178.76(19)	C2---C1---C9---C10	-176.90(19)
C1---C9---C10---C11	-159.1(2)	C2---C1---C9---C13	66.6(3)
C1---C9---C13---C12	155.9(2)	C2---C3---C4---C5	178.5(2)

Table 3
Hydrogen bond interactions for $C_{13}H_{15}N_2Cl$ (**6a**) [Å and °].

D–H...A	d(D–H) (Å)	d(H–A) (Å)	d(D–A) (Å)	D–H–A (°)
N1---H1...N2[a]	0.88	2.04	2.890(2)	162
C1---H1A...N2[b]	0.99	2.81	3.485(3)	126.1

Symmetry transformations used to generate equivalent atoms:
[a] $+X, 3/2 - Y, -1/2 + Z$.
[b] $1 - X, 1 - Y, 1 - Z$.

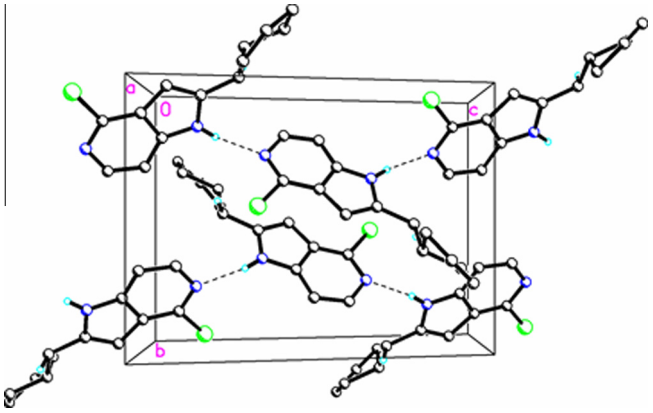

Fig. 3. Packing diagram of $C_{13}H_{15}N_2Cl$ (**6a**) viewed along the *a* axis. Dashed lines indicate N---H...N hydrogen bonds, which link the molecules into chains along [001]. H atoms not involved in hydrogen bonding have been deleted for clarity.

dilutions of the synthesized compounds and reference compound were added to the wells (750, 700, 650...25 μg/mL). Then a suspension of microorganism was inoculated into the wells. Final inoculums concentrations in the wells were 100 cfu/mL. The plates were incubated at 37 °C for 24 h for the antibacterial activity. At the end of the incubation period, MIC values were recorded as the lowest concentration of the substances that has no visible turbidity.

Molecular docking study procedure

The protein-drug interaction was studied by automated docking to determine the orientation of inhibitors bound to the active site of target protein GlcN-6-P synthase. A genetic algorithm method, implemented in the program AutoDock 4.2, was employed [28]. The 2D structures (.mol) of all the six compounds are converted to 3D structure (.pdb) using Openbable software tool. The 3D coordinates (.pdb) of each molecule were loaded on to PRODRG server [29] and PreADMET server for energy minimization and drug-likeliness prediction respectively. The protein structure file 1Jxa was downloaded from Protein Data Bank (www.rcsb.org/pdb) was edited by removing the heteroatom's, adding C-terminal oxygen [30]. For docking calculations, Gasteigere Marsili partial charges [31] were assigned to the inhibitors and non-polar hydrogen atoms were merged. All torsions were allowed to rotate during docking. The grid map was centered at the residues of the protein, predicted from the CASTp server [32]. The Lamarckian genetic algorithm and the pseudo-Solis and Wets methods were applied for minimization using default parameters. The number of docking runs was 50, the population in the genetic algorithm was 250, the number of energy evaluations was 100,000, and the maximum number of iterations 10,000. The docking results for inhibitors against glucosamine-6-phosphate synthase [PDB Id: 1jka], showed minimum docking energy, inhibition constant, with RMS as documented. The computer specification used-Operating system: Microsoft Windows XP, Processor: Intel Pentium 3.40 GHz, RAM: 2 GB, Hard disk: 500 GB, Python: 2.4.

Results and discussion

Chemistry

We describe here an efficient method for the synthesis of novel pyrrolo[3,2-c]pyridine derivatives (**6a–c**, **7a–f**) (Scheme 1). The commercially available **1** (2-Chloro-4-amino pyridine) was iodinated with ICl and KOAc in glacial acetic acid at 70 °C to afford a mixture of iodopyridines **2** (2-chloro-3-iodopyridin-4-amine), **3** (2-chloro-5-iodopyridin-4-amine) and **4** (2-chloro-3,5-diiodopyridin-4-amine) in the ratio 45:45:10 [17]. The iodopyridines were

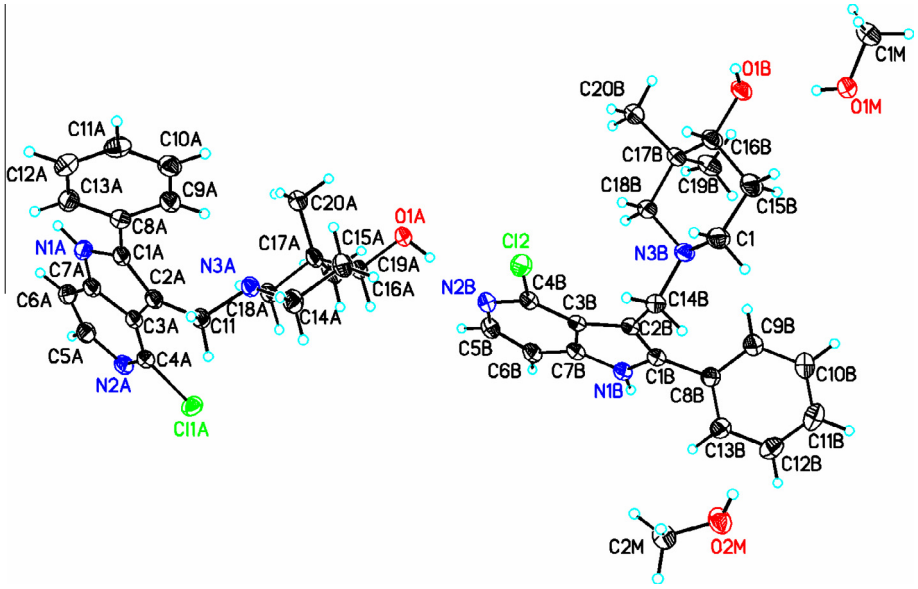

Fig. 4. Molecular structure of $C_{21}H_{24}N_3OCl$, CH_4O (**7c**) showing the atom labeling scheme and 30% probability displacement ellipsoids.

Table 4
Selected Crystal Bond lengths (Å), Bond angles (°), and Torsion angles (°) for $C_{21}H_{24}N_3OCl$, CH_4O (**7c**).

$C_{21}H_{24}N_3OCl$, CH_4O			
Cl1A---C4A	1.749(2)	N1B---C1B	1.380(3)
Cl2---C4B	1.744(3)	N1B---C7B	1.353(3)
O1A---C16A	1.434(3)	N2A---C4A	1.309(3)
O1B---C16B	1.427(3)	N2A---C5A	1.364(3)
O1M---C1M	1.419(3)	N2B---C4B	1.314(3)
O2M---C2M	1.411(3)	N2B---C5B	1.354(3)
N1A---C1A	1.382(3)	N3A---C11	1.474(3)
N1A---C7A	1.360(3)	N3A---C14A	1.455(3)
$C_{21}H_{24}N_3OCl$, CH_4O			
C7A---N1A---C1A	108.80(19)	C18B---N3B---C1	110.67(19)
C7B---N1B---C1B	109.3(2)	C18B---N3B---C14B	111.82(18)
C4A---N2A---C5A	117.9(2)	N3B---C1---C15B	110.8(2)
C4B---N2B---C5B	118.2(2)	N1A---C1A---C8A	119.4(2)
C14A---N3A---C11	110.31(18)	C2A---C1A---N1A	110.0(2)
C18A---N3A---C11	112.59(17)	C2A---C1A---C8A	130.5(2)
C18A---N3A---C14A	110.37(19)	N1B---C1B---C8B	120.3(2)
C1---N3B---C14B	109.22(18)	C2B---C1B---N1B	109.9(2)
$C_{21}H_{24}N_3OCl$, CH_4O			
O1A---C16A---C17A---C18A	−178.32(18)	N1A---C1A---C8A---C9A	−145.3(2)
O1A---C16A---C17A---C19A	64.7(3)	N1A---C1A---C8A---C13A	36.1(3)
O1A---C16A---C17A---C20A	−57.5(3)	N1B---C1B---C2B---C3B	1.0(3)
O1B---C16B---C17B---C18B	179.98(19)	N1B---C1B---C2B---C14B	177.9(2)
O1B---C16B---C17B---C19B	58.7(3)	N1B---C1B---C8B---C9B	142.1(2)
O1B---C16B---C17B---C20B	−63.3(3)	N1B---C1B---C8B---C13B	−39.1(3)
N1A---C1A---C2A---C3A	0.0(2)	N2A---C5A---C6A---C7A	2.7(4)
N1A---C1A---C2A---C11	−179.50(19)	N2B---C5B---C6B---C7B	−0.9(4)

isolated by preparative HPLC (normal phase). The structures of iodopyridines were assigned on the basis of ^{1}H NMR, mass spectral analysis and elemental analysis. ^{1}H NMR spectrum of elution 1 (**4**) showed two singlet peaks at δ 8.17 and 6.51 ppm corresponds to aromatic hydrogen at C6 and NH_2 group; elution 2 (**3**) showed three singlet peaks at δ 8.18, 6.65, 6.50 ppm corresponds to aromatic protons at C3, C6 and NH_2 group, whereas elution 3 (**2**) showed two doublet peaks and a single peak at δ 7.73, 6.52 and 6.50 corresponds to aromatic protons at C5, C6 and NH_2 group. The 2-amino-3-iodo pyridine (**2**) were refluxed in THF with a catalytic amount of Bis(triphenylphosphine)palladium(II) dichloride, copper (I) iodide, triethylamine as a base and acetylenes to afford desired compounds (**5a**–**c**) [33]. The formation of pyrrole ring was accomplished by treatment of **5** with potassium tert butoxide and NMP at 100 °C [34] afford compounds (**6a**–**c**). The final

Table 5
Hydrogen bond interactions for $C_{21}H_{24}N_3OCl$, CH_4O (**7c**) [Å and °].

D–H...A	d(D–H) (Å)	d(H–A) (Å)	d(D–A) (Å)	D–H–A (°)
O1A---H1A...N2B	0.87(3)	1.92(3)	2.774(3)	171(3)
O1B---H1B...N2A[a]	0.80(3)	1.98(3)	2.775(3)	176(3)
O1M---H1M...O1B	0.81(3)	1.88(3)	2.678(3)	170(3)
O2M---H2M...O1A[b]	0.79(4)	1.91(4)	2.702(3)	176(4)
N1A---H1AA...O1M[c]	0.88	1.94	2.778(3)	159.8
N1B---H1BA...O2M[d]	0.88	1.92	2.749(3)	155.7
C9A---H9A...N3A	0.95	2.39	3.217(3)	144.8
C9B---H9B...N3B	0.95	2.51	3.293(3)	140.1

Symmetry transformations used to generate equivalent atoms:
[a] *X*, +*Y*, −1 + *Z*.
[b] 1 − *X*, 1 − *Y*, 1 − *Z*.
[c] 1 + *X*, +*Y*, 1 + *Z*.
[d] −*X*, 1 − *Y*, 1 − *Z*.

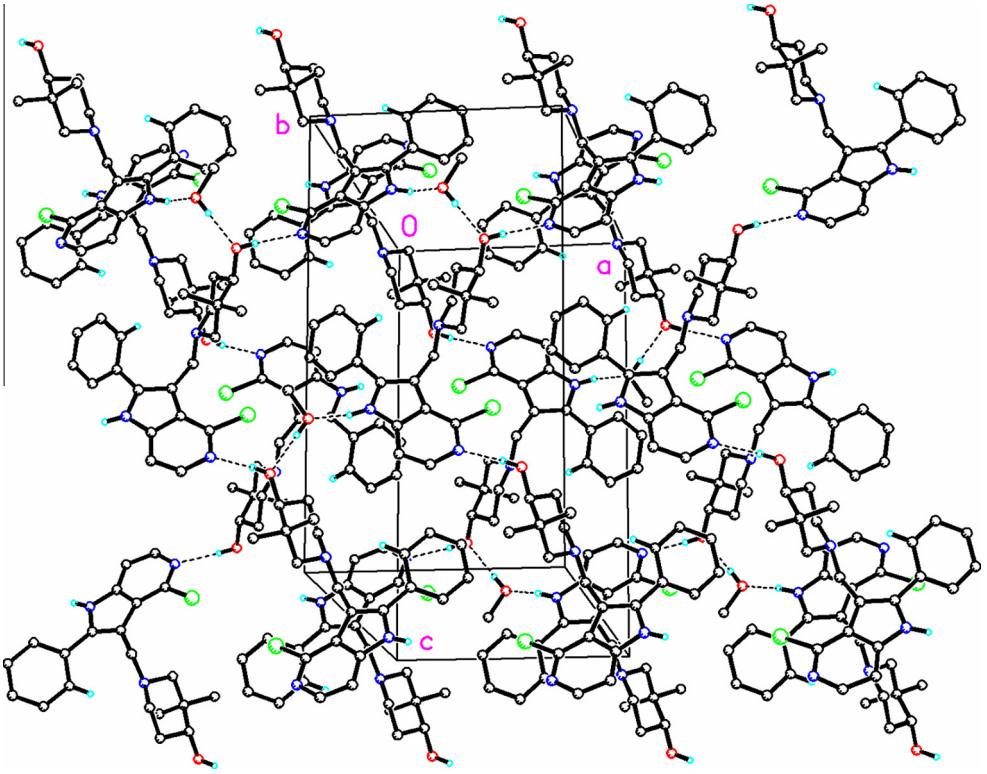

Fig. 5. Packing diagram of $C_{21}H_{24}N_3OCl$, CH_4O (**7c**) viewed along the *b* axis. Dashed lines indicate O---H...N, O---H...O, N---H...O hydrogen bonds and weak C---H...N intermolecular interactions, which link the molecules into a two-dimensional network along (0 1 0). H atoms not involved in hydrogen bonding have been deleted for clarity.

Table 6
Antibacterial and antifungal activity of **6a–c**, **7a–f**.

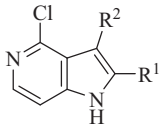

Compound	R^1	R^2	Bacteria		Fungus	
			Pseudomonas spp.	*Bacillus flexus*	*Scopulariopsis* spp.	*Aspergillus tereus*
6a	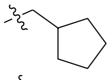		–	–	–	–
6b			–	–	–	–
6c	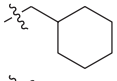		–	–	–	–
7a	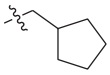		–	+++	–	–
7b		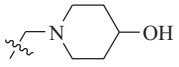	–	++	–	–
7c		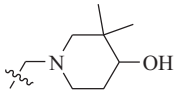	–	++	–	–
7d	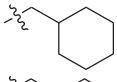	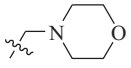	–	++++	–	–
7e	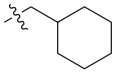	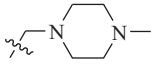	–	+++++	–	–

(*continued on next page*)

Table 6 (*continued*)

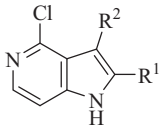

Compound	R^1	R^2	Bacteria		Fungus	
			Pseudomonas spp.	*Bacillus flexus*	*Scopulariopsis* spp.	*Aspergillus tereus*
7f	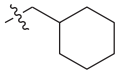	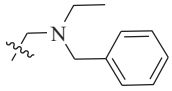	–	++++	–	–
Amoxycillin	–	–	+++++	+++++	–	–
Nystatin	–	–	–	–	+++++	+++++

Zone of inhibition in mm; +++++ = 32 mm, ++++ = 20 mm, +++ = 15 mm, ++ = 10 mm, hyphen denotes no activity.

compounds (**7a**–**f**) were synthesized in 88–94% yield via Mannich reaction of **6**, a secondary amine, and formaldehyde in glacial acetic acid. All the final products, except **7c** are achiral and the structures were assigned on the basis of their ^{1}H NMR, ^{13}C NMR and mass (LCMS or HRMS) spectral analysis as well as elemental analysis.

Table 7
Antibacterial activity MIC (μg/mL) of compounds **7a**–**f**.

Compound	Structure	MIC (μg/mL) *Bacillus flexus*	LogP
7a	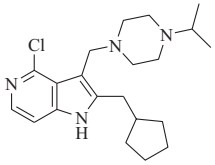	300	4.363
7b	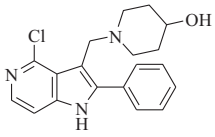	700	2.297
7c	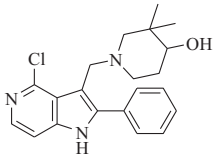	650	3.551
7d	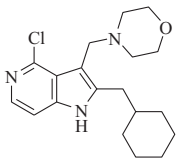	200	4.151
7e	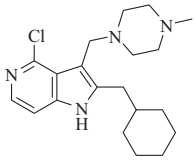	50	4.196
7f	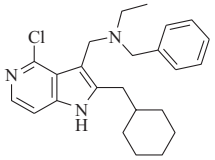	150	6.079
Amoxicillin	–	25	−1.352

X-ray crystal structure analysis

*4-Chloro-2-(cyclopentylmethyl)-1H-pyrrolo[3,2-c]pyridine (**6a**)*

In $C_{13}H_{15}N_2Cl$, one independent molecule crystallizes in the asymmetric unit (Fig. 2). The five-membered cyclopentane ring adopts a slightly distorted envelope conformation (q = 0.358(3) Å, ϕ = 3.0(5)°) [35] with the carbon atom attached to the methylene group. The nine-membered pyrrolo[3,2-c]pyridine ring is planar with the maximum deviation of −0.0026(17) Å and −0.0034(18) Å from the mean plane by N1 and N2, respectively. Bond angles and distances are in normal ranges [36] (Table 2). In the crystal, N1---H1...N1 hydrogen bonds are observed (Table 3) which link the molecules into one-dimensional chains along [001] (Fig. 3).

*1-((4-Chloro-2-phenyl-1H-pyrrolo[3,2-c]pyridin-3-yl)methyl)-3,3-dimethylpiperidin-4-ol compound with methanol (**7c**)*

The compound **7c** is racemic mixture and crystallizes in a centrosymmentric space group $P\bar{1}$. In $C_{21}H_{24}N_3OCl$, CH_4O, two independent compound molecules (A & B) and two independent methanol solvent molecules crystallize in the asymmetric unit (Fig. 4). In the compound the 6-membered piperidine ring adopts a slightly distorted chair conformation (puckering parameters (A) q, θ, and ϕ = 0.578 (3) Å, 177.6 (2)° and 154 (2)°; (B) q, θ, and ϕ = 0.584 (3) Å, 0.0 (3)° and 291 (2)°) [35]. Bond angles and distances are in normal ranges [36] (Table 4). The dihedral angles between the mean planes of the nine-membered pyrrolo[3,2-c]pyridin-3-yl and six-membered phenyl rings are 39.5(8)° (A) and 42.28° (B), respectively. In the asymmetric unit hydrogen bonds between the hydroxy group and pyridine ring of the compound (O1A---H1A...N2B) and methanol solvent group with the hydroxyl group of the compound (O1M---H1M...O1B) are observed. Also, O---H...N intermolecular hydrogen bonds involving the compound and N---H...O, O---H...O hydrogen bonds between the compound and methanol solvent molecule are present (Table 5). These intermolecular interactions in addition to weak C---H...N intermolecular interactions generate an infinite two-dimensional network along the (010) plane (Fig. 5).

Antimicrobial activity

The title compounds were tested for their antimicrobial activity against Gram-positive bacteria *B. flexus*, Gram-negative bacteria *Pseudomonas* spp., fungal stains *Scopulariopsis* spp. and *A. tereus*. Amoxicillin and Nystatin were used as antibacterial and antifungal references, respectively. As shown in Table 6, six compounds **(7a–f)** showed antibacterial activity against *B. flexus* (Gram-positive bacteria) and no activity against Gram-negative bacteria. The com-

pounds showed no antifungal activity against both *Scopulariopsis* spp. and *A. tereus*.

Six compounds from the above result were tested for antibacterial activity (MIC) against *B. flexus*. The synthesized compounds **(7a–f)** exhibited a broad spectrum activity with MIC values of 50–700 μg/mL against the gram-positive bacteria *B. flexus* (Table 7). The compound **7e** gave the best inhibitory activity with MIC 50 μg/mL. The compounds **7b** and **7c** were required in higher amounts to inhibit the activity of the organism in the study. Compound **7c** is a mixture of enantiomers gave the modest inhibitory activity with MIC 650 μg/mL. Lipophilicities of the compounds **7a-f**, which were expressed as log*P*, was determined using the logP method through online http://www.molinspiration.com/cgi-bin/properties site, as shown in Table 7. At this stage, some structure–activity relationships could be concluded from the data described in Table 7. As a result, pyrrolo[3,2-c]pyridines that carry aliphatic substituent's such as cyclohexylmethyl and cyclopentylmethyl at position 2, were found to be more potent as antimicrobial agents compared to compounds carrying phenyl substituent at position 2.

Molecular docking studies

The new pyrrolopyridines were predicted for drug-likeliness property using PreADMET server [37,38]. To explain the

Table 8
Molecular docking of pyrrolo[3,2-c]pyridine motifs with GlcN-6-P synthase.

Compound	Docking energy (kcal/mol)	Binding energy (kcal/mol)	Intermolecular energy (kcal/mol)	Inhibition constant (M)	RMSD (Å)	Hydrogen bonds	Bonding	Bond length (Å)
7a	−12.22	−10.98	−12.30	1.52×10^{-8}	0.71	2	**7a**:NH:::OH:Pro377 **7a**:NH:::OH:Gly378	2.92 2.60
7b	−11.48	−10.18	−11.60	1.87×10^{-8}	0.80	0	–	–
7c	−10.76	−10.39	−10.91	6.31×10^{-8}	0.99	2	**7c**:HO:::HOOC:Pro377 **7c**:NH:::OH:Tyr25	2.86 2.56
7d	−11.30	−10.22	−11.42	4.25×10^{-8}	0.82	0	–	–
7e	−10.40	−8.81	−10.49	1.41×10^{-7}	1.02	0	–	–
7f	−10.89	−8.89	−10.99	4.10×10^{-7}	0.96	1	**7f**:NH:::OH:Tyr25	2.87

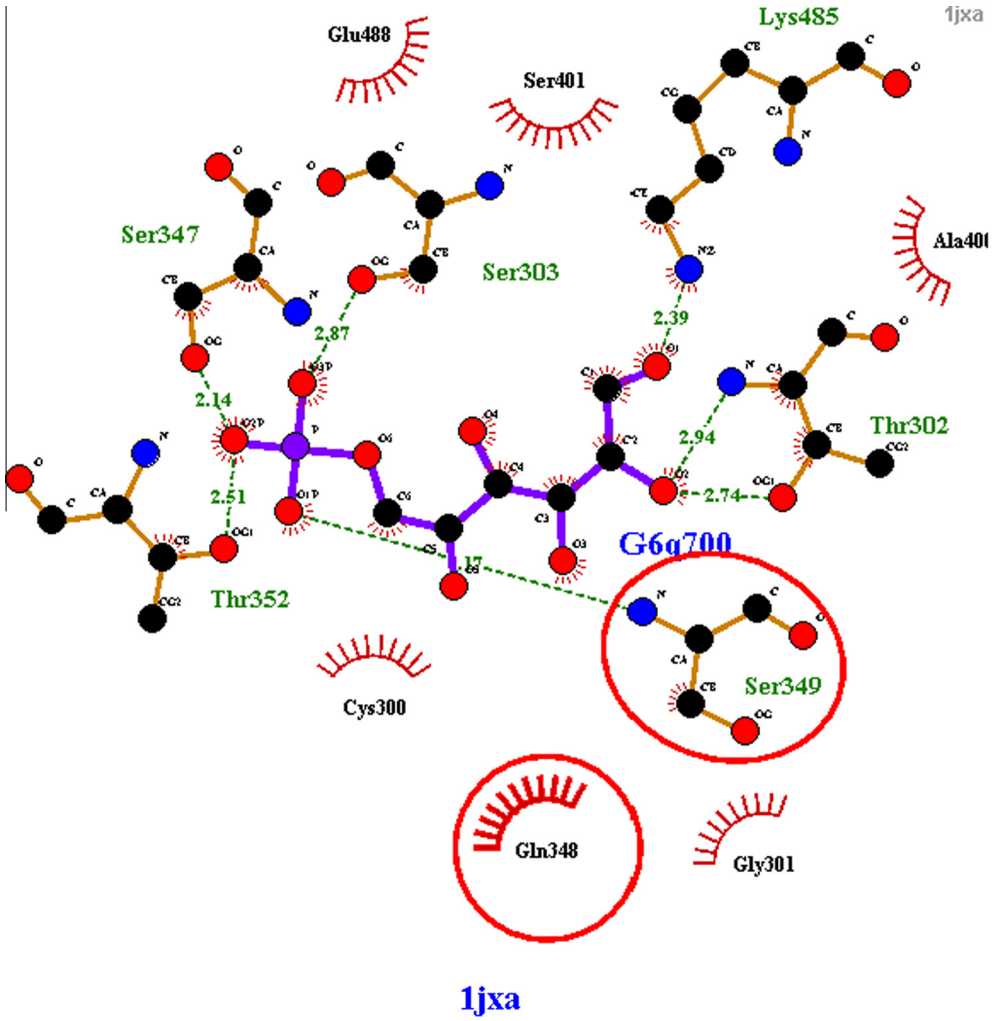

Fig. 6. Ligplot of GlcN-6-P showing the binding of glucosamine-6-phosphate in an active site of enzyme.

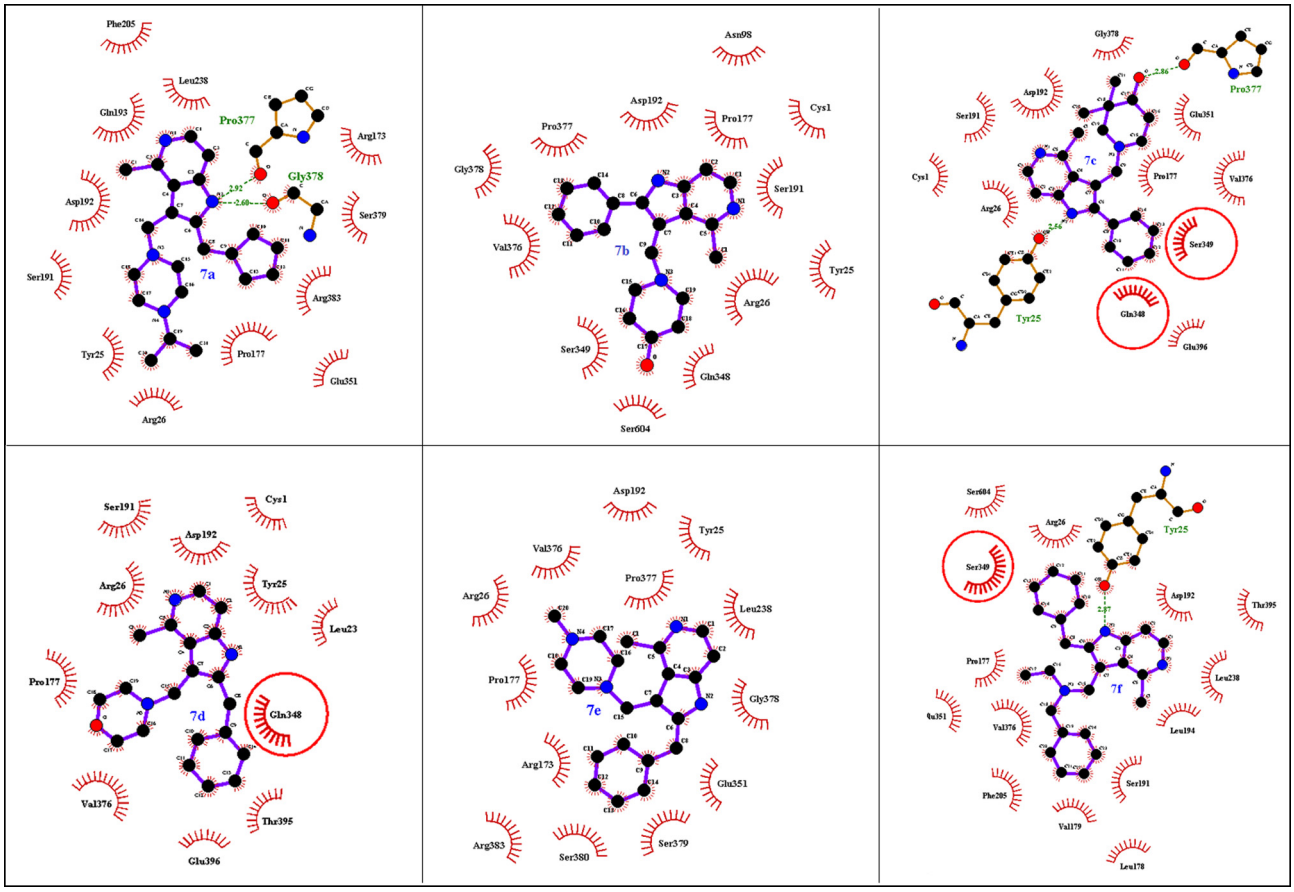

Fig. 7. Ligplot images of protein ligand interactions of **7a–f** with GlcN-6-P synthase.

antibacterial activity of new pyrrolopyridines, we explore the binding affinity of the compounds against Glucosamine-6-phosphate synthase, the target enzyme for the antimicrobial agents. The molecular docking of the GlcN-6-P synthase with **7a–f** and the standard drug fluconazole yielded best possible conformations with parameters including the docking energy, binding energy, intermolecular energy, inhibition constant and RMSD (Table 8). The topology of the active site of GlcN-6-P synthase was similar in both pyrrolopyridines and fluconazole, which is lined by interacting amino acids as predicted from the ligplot. The binding pocket of GlcN-6-P synthase contains the following amino acid residues, Cys300, Gly301, Thr302, Ser303, Ser347, Gln348, Ser349, Thr352, Val399, Ser401, Ala602 and Lys603 (Fig. 6). Fig. 7 illustrates the protein ligand interactions of pyrrolopyridines with GlcN-6-P synthase. Theoretically, all the six compounds (**7a–f**) showed very good docking energy ranging from −10.40 kcal/mol to −12.22 kcal/mol. Compounds **7a**, **7c** and **7f** have formed hydrogen bonds with the active site of the GlcN-6-P synthase. All target compounds (**7a–f**) containing chlorine as halogen atom have formed intermolecular bonds with the active site of the GlcN-6-P synthase in a fashion that resembles the H bonds [39–41]. Compounds containing the halogen atoms will also improve the oral absorption, skin penetration and also increase membrane permeability [42].

The minimum docking energy was found in the analogue **7a** (−12.22 kcal/mol) with an estimated inhibition constant of 1.52×10^{-8} M, binding energy −10.98 kcal/mol, intermolecular energy −12.3 kcal/mol and RMSD (root-mean square deviation) 0.71 Å. Whereas, the docked energy of the standard drug fluconazole was −5.67 kcal/mol with an inhibition constant of 5.53×10^{-5} M and RMSD 1.97 Å. The NH group of **7a** has formed two hydrogen bonds with a hydroxy group of amino acid residues at the active site of the GlcN-6-P synthase, Pro377 (2.92 Å) and Gly378 (2.6 Å), respectively. In *in vitro* antimicrobial study compound **7a** emerged as active against *B. flexus*, so it can be predicted as the activity may be due to inhibition of enzyme GlcN-6-Psynthase, which catalyses a complex reaction involving ammonia transfer from L-glutamine to Fru-6-P followed by isomerisation of the formed fructosamine-6-phosphate to glucosamine-6-phosphate. The accuracy of dockings was evaluated by the RMSD of the docked ligand from original crystal structure. RMSD less than 1.0 Å was considered as excellent. Compound **7c** forms two hydrogen bonds with amino acid residues in the active site of the GlcN-6-P synthase. The hydroxy group of **7c** forms a hydrogen bond with COOH of Pro377 (2.86 Å) and the NH of **7c** also forms a hydrogen bond with the OH of Tyr25 (2.56 Å). In solid state of **7c**, O---H...N intermolecular hydrogen bonds between the hydroxy group and pyridine ring of the compound, N---H...O, O---H...O hydrogen bonds between the compound and methanol solvent molecule and weak C---H...N intermolecular interactions were observed (Table 5). This intermolecular hydrogen bonding interaction observed in solid state was further strengthened the binding capability of the compound **7c** and the active sites were NH, OH groups and pyridine ring. The docking study reveals that the high affinity of pyrrolopyridine derivatives (**7a–f**) within the binding pocket of GlcN-6-P synthase strongly enhanced the determined activities of these derivatives as potent antimicrobial agents.

Conclusions

In summary, we have synthesized new antibacterial leads **(7a**, **7d**, **7e** and **7f)** with moderate to good activity against Gram-posi-

tive bacteria *B. flexus* compared to the control antibiotic amoxicillin. The compound **7e** gave the best inhibitory activity with MIC 50 μg/mL. The structure-antimicrobial activity relationship of these derivatives was explained by molecular docking. Two of these (**6a**, **7c**) were obtained as single crystals and their crystal structures were studied. The results described here, merit further investigations in our laboratories for finding anti-infective agents.

Acknowledgements

The authors are thankful to the authorities of Jain University for encouragement and financial support for this work. GJ acknowledges the NMR Research Centre, Indian Institute of Science, Bangalore, for providing spectral data. JPJ acknowledges the NSF-MRI program (Grant No: CHE-1039027) for funds to purchase the X-ray diffractometer.

Appendix A. Supplementary material

CCDC 992274 and 992275 contains the supplementary crystallographic data for $C_{13}H_{15}N_2Cl$ and $C_{21}H_{24}N_3OCl$, CH_4O. These data can be obtained free of charge via http://www.ccdc.cam.ac.uk/conts/retrieving.html, or from the Cambridge Crystallographic Data Centre, 12, Union Road, Cambridge CB2 1EZ, UK; fax: (+44) 1223 336 033; or email: deposit@ccdc.cam.ac.uk. Supplementary data associated with this article can be found, in the online version, at http://dx.doi.org/10.1016/j.molstruc.2014.10.006. These data include MOL files and InChiKeys of the most important compounds described in this article.

References

[1] S.R. Walker, E.J. Carter, B.C. Huff, J.C. Morris, Chem. Rev. 109 (2009) 3080–3098.
[2] M. Prudhomme, Eur. J. Med. Chem. 38 (2003) 123–140.
[3] B. Nowicka-Sans, Y.-F. Gong, B. McAuliffe, I. Dicker, H.-T. Ho, N. Zhou, B. Eggers, P.-F. Lin, N. Ray, M. Wind-Rotolo, L. Zhu, A. Majumdar, D. Stock, M. Lataillade, G.J. Hanna, J.D. Matiskella, Y. Ueda, T. Wang, J.F. Kadow, N.A. Meanwell, M. Krystal, Antimicrob. Agents Chemother. 56 (2012) 3498–3507.
[4] J.R. Henry, K.C. Rupert, J.H. Dodd, I.J. Turchi, S.A. Wadsworth, O.E. Cavender, B. Fahmy, G.C. Olini, J.E. Davis, J.L. Pellegrino, P.H. Schafer, J.J. Siekierka, J. Med. Chem. 41 (1998) 4196–4198.
[5] J.I. Manchester, D.D. Dussault, J.A. Rose, P.A.B. Sjodin, M.U. Nickelsen, G. Ioannidis, S. Bist, P. Fleming, K.G. Hull, Bioorg. Med. Chem. Lett. 22 (2012) 5150–5166.
[6] T.C. Leboho, S.F. Vuuren, J.P. Michael, C.B. Koning, Org. Biomol. Chem. 12 (2014) 307–315.
[7] K. Kumaran, S.R.M. Kamil, K.R. Jaisankar, Int. J. Pharm. Tech. Res. 4 (2012) 169–175.
[8] S.D. Paget, C.M. Boggs, B.D. Foleno, R.M. Goldschmidt, D.J. Hlasta, M.A. Weidner-Wells, H.M. Werblood, K. Bush, M.J. Macielag, Bioorg. Med. Chem. Lett. 16 (2006) 4537–4542.
[9] J.I. Manchester, D.D. Dussault, J.A. Rose, P.A. Boriack-Sjodin, M. Uria-Nickelsen, G. Ioannidis, S. Bist, P. Fleming, K.G. Hull, Bioorg. Med. Chem. Lett. 22 (2012) 5150–5156.
[10] N. Mushtaq, Z.S. Saify, F. Noor, S. Takween, S. Akhtar, M. Arif, K.M. Khan, Pak. J. Pharm. Sci. 21 (2008) 36–39.
[11] A.J. Verbiscar, J. Med. Chem. 15 (1972) 149–152.
[12] C. Marminon, A. Pierre, B. Pfeiffer, V. Perez, S. Leonce, A. Joubert, C. Bailly, P. Renard, J. Hickman, M. Prudhomme, J. Med. Chem. 46 (2003) 609–622.
[13] M.R. Bell, J.O. Hoppe, H.E. Lape, D. Wood, A. Arnold, W.H. Selberis, Cell. Mol. Life Sci. 23 (1967) 298–299.
[14] A.R. Blaazer, J.H.M. Lange, M.A.W.V. Neut, A. Mulder, F.S.D. Boon, T.R. Werkman, C.G. Kruse, W.J. Wadman, Eur. J. Med. Chem. 46 (2011) 5086–5098.
[15] G.M.P. Giblin, A. Billinton, M. Briggs, A.J. Brown, I.P. Chessell, N.M. Clayton, A.J. Eatherton, P. Goldsmith, C. Haslam, M.R. Johnson, W.L. Mitchell, A. Naylor, A. Perboni, B.P. Slingsby, A.W. Wilson, J. Med. Chem. 52 (2009) 5785–5788.
[16] H. Hu, A. Kolesnikov, J.R. Riggs, K.E. Wesson, R. Stephens, E.M. Leahy, W.D. Shrader, P.A. Sprengeler, M.J. Green, E. Sanford, M. Nguyen, E. Gjerstad, R. Cabuslay, W.B. Young, Bioorg. Med. Chem. Lett. 16 (2006) 4567–4570.
[17] G. Jose, T.H.S. Kumara, G. Nagendrappa, H.B.V. Sowmya, J.P. Jasinski, S.P. Millikan, N. Chandrika, S.S. More, B.G. Harish, Eur. J. Med. Chem. 77 (2014) 288–297.
[18] D.T.W. Chu, J.J. Plattner, L. Katz, J. Med. Chem. 39 (1996) 3853–3874.
[19] J. Davies, Nature 383 (1996) 219–220.
[20] C.A. Hitchock, Biochem. Soc. Trans. 21 (1993) 1039–1047.
[21] F.C. Odds, J. Antimicrob. Chemother. 31 (1993) 463–471.
[22] S. Milewski, Biochim. Biophys. Acta 1597 (2002) 173–192.
[23] O.V. Dolomanov, L.J. Bourhis, R.J. Gildea, J.A.K. Howard, H. Puschmann, J. Appl. Cryst. 42 (2009) 339–341.
[24] L. Palatinus, G. Chapuis, J. Appl. Cryst. 40 (2007) 786–790.
[25] G.M. Sheldrick, Acta Cryst. A64 (2008) 112–122.
[26] B.A. Arthington-Skaggs, M. Motley, D.W. Warnock, C.J. Morrison, J. Clin. Microbiol. 38 (2000) 2254–2260.
[27] J.M. Swenson, G.E. Killgore, F.C. Tenover, J. Clin. Microbiol. 42 (2004) 5102–5108.
[28] G.M. Morris, R. Huey, W. Lindstrom, M.F. Sanner, R.K. Belew, D.S. Goodsell, A.J. Olson, J. Comp. Chem. 16 (2009) 2785–2791.
[29] A.K. Ghose, G.M. Crippen, J. Chem. Inform. Comput. Sci. 27 (1987) 21–35.
[30] T.A. Binkowski, S. Naghibzadeg, J. Liang, Nucleic Acids Res. 31 (2003) 3352–3355.
[31] J. Gasteiger, M. Marsili, Tetrahedron 36 (1980) 3219–3228.
[32] T. Reya, H. Clevers, Nature 434 (2005) 843–850.
[33] S. Yagai, S. Mahesh, Y. Kikkawa, K. Unoike, T. Karatsu, A. Kitamura, A. Ajayaghosh, Angew. Chem. Int. Ed. Engl. 47 (2008) 4691–4694.
[34] C. Koradin, W. Dohle, A.L. Rodriguez, B. Schmid, P. Khochel, Tetrahedron 59 (2003) 1571–1587.
[35] D. Cremer, J.A. Pople, J. Am. Chem. Soc. 97 (1975) 1354–1358.
[36] F.H. Allen, O. Kennard, D.G. Watson, L. Brammer, A.G. Orpen, R. Taylor, J. Chem. Soc. Perkin Trans. 2 (1987) S1–S19.
[37] D.E. Clark, Drug Discovery Today 8 (2003) 927–933.
[38] R. Didziapetris, P. Japertas, A. Avdeef, A.J. Petrauskas, Drug Target 11 (2003) 391–406.
[39] S. Buchini, A. Buschiazzo, S.G. Withers, Angew. Chem. Int. Ed. Engl. 47 (2008) 2700–2703.
[40] C. Bonnefous, J.E. Payne, J. Roppe, H. Zhuang, X. Chen, K.T. Symons, P.M. Nguyen, M. Sablad, N. Rozenkrants, Y. Zhang, L. Wang, D. Severance, J.P. Walsh, N. Yazdani, A.K. Shiau, S.A. Noble, P. Rix, T.S. Rao, C.A. Hassig, N.D. Smith, J. Med. Chem. 52 (2009) 3047–3062.
[41] A.C. Leite, D.R. Moreira, M.V. Cardoso, M.Z. Hernandes, V.R.A. Pereira, R.O. Silva, A.C. Kiperstok, S.L. Mda, M.B. Soares, ChemMedChem 2 (2009) 1339–1345.
[42] C.L. Gentry, R.D. Egleton, T. Gillespie, T.J. Abbruscato, H.B. Bechowski, V.J. Hruby, T.P. Davis, Peptides 20 (1999) 1229–1238.